The Journal of Experimental Biology **199**, 985–997 (1996)
Printed in Great Britain © The Company of Biologists Limited 1996
JEB0238

THE MECHANICAL PROPERTIES OF FIN WHALE ARTERIES ARE EXPLAINED BY NOVEL CONNECTIVE TISSUE DESIGNS

JOHN M. GOSLINE[1] AND ROBERT E. SHADWICK[2]

[1]*Department of Zoology, University of British Columbia, Vancouver, BC, Canada V6T 1Z4* and [2]*Marine Biology Research Division, Scripps Institution of Oceanography, La Jolla, CA 92093-0204, USA*

Accepted 15 December 1995

Summary

The aortic arch and the descending aorta in the fin whale (*Balaenoptera physalus*) are structurally and mechanically very different from comparable vessels in other mammals. Although the external diameter of the whale's descending thoracic aorta (approximately 12 cm) is similar to that predicted by scaling relationships for terrestrial mammals, the wall thickness:diameter ratio in the whale (0.015) is much smaller than the characteristic value for other mammals (0.05). In addition, the elastic modulus of the thoracic aorta (12 MPa at 13 kPa blood pressure) is about 30 times higher than in other mammals. In contrast, the whale's aortic arch has a wall thickness/diameter ratio (0.055) and an elastic modulus (0.4 MPa) that are essentially identical to those for other mammals. However, the aortic arch is unusual in that it can be deformed biaxially to very large strains without entering a region of high stiffness caused by the recruitment of fully extended collagen fibres. Chemical composition studies indicate that the elastin:collagen ratio is high in the aortic arch (approximately 2:1) and that this ratio falls in the thoracic (approximately 1:2) and abdominal (approximately 1:3) aortas, but the magnitude of the change in composition does not account for the dramatic difference in mechanical properties. This suggests that there are differences in the elastin and collagen fibre architecture of these vessels. The descending aorta contains dense bands of tendon-like, wavy collagen fibres that run in the plane of the arterial wall, forming a fibre-lattice that runs in parallel to the elastin lamellae and reinforces the wall, making it very stiff. The aortic arch contains a very different collagen fibre-lattice in which fibres appear to have a component of orientation that runs through the thickness of the artery wall. This suggests that the collagen fibres may be arranged in series with elastin-containing elements, a difference in tissue architecture that could account for both the lower stiffness and the extreme extensibility of the whale's aortic arch. Thus, both the structure and the mechanical behaviour of the lamellar units in the aortic arch and aorta of the whale have presumably been modified to produce the unusual mechanical and haemodynamic properties of the whale circulation.

Key words: fin whale, *Balaenoptera physalus*, aortic arch, aorta, elastic modulus, lamellar unit, collagen, elastin.

Introduction

The arterial system of mammals is constructed so that the elastic properties and the dimensions of the major arteries are matched to cardiac frequency in a way that allows the propagation and reflection of pressure waves to minimize the load on the heart (Milnor, 1982). Typically, the central components of this system, the aortic arch and the thoracic and abdominal aortas, are highly distensible pressure vessels that gradually decrease in size (geometric taper) and gradually increase in stiffness (elastic taper) with distance away from the heart, and the precise taper of the central arteries creates a wave-propagation system that allows pressure waves reflected from peripheral reflecting sites to arrive at the heart approximately one half-cycle out of phase with the next outgoing pressure wave. Thus, reflected waves combine destructively with outgoing waves to lower the pressure against which the heart must work. Typically, the circumferential elastic modulus at *in vivo* pressure rises by a factor of four from the arch to the distal abdominal aorta, and arterial diameter at *in vivo* pressure decreases by about 50 % over the same distance.

Diving mammals show a modification of this general pattern in that the aortic arch is significantly enlarged relative to the thoracic aorta, forming a structure commonly called the aortic bulb, and this modification is thought to alter the haemodynamics of the central circulation as an adaptation for diving (Drabek, 1975; Shadwick and Gosline, 1995). Recently, the arterial haemodynamics of the fin whale was evaluated through an analysis of the mechanical properties of its major arteries (Shadwick and Gosline, 1994), and it was discovered that there is a major discontinuity between the aortic arch and

the thoracic aorta. That is, the gradual taper characteristic of terrestrial mammals is replaced by a dramatic rise in the elastic modulus of the arterial wall material and a dramatic drop in arterial diameter at the transition between the aortic arch and the thoracic aorta.

The haemodynamic consequence of this abrupt transition is that there is a strong impedance mis-match between the aortic arch and the thoracic aorta that effectively decouples the arch from the remainder of the caudal arterial tree. The low-stiffness, large-diameter aortic arch functions as a central windkessel that provides the majority of the arterial capacitance for the whale, and the high-stiffness thoracic and abdominal aortas function largely as rigid conduits that provide little capacitance and are not likely to be tuned to return pressure waves that will combine destructively at the aortic arch. Although these modifications to the major arteries appear to be correlated with the requirements of diving, the fin whale and its relatives are the largest animals in existence (approximately 40 000 kg body mass), and these modifications may also reflect the requirements of large body size.

The purpose of the current study is to determine the nature of the structural modifications that have occurred during the evolution of the whale's central arterial system to create these unusual properties. Typically, the wall of the mammalian aorta is an elastic tissue that contains three major components: (1) the rubber-like protein elastin, (2) the rigid, fibrous protein collagen, and (3) smooth muscle cells that synthesize the elastin and collagen and also provide a degree of active control of wall mechanical properties. These three components are found in thin layers that are arranged in repeating lamellar units, each of which is about 15 μm thick, that contain thin layers of elastin and collagen and a thick layer of smooth muscle cells (Wolinsky and Glagov, 1964, 1967; Rodin, 1980; Clark and Glagov, 1985). The elastin lamellae and collagen fibres run parallel to each other and to the cells, but the collagen and elastin do not appear to be linked together. The lamellar units are arranged concentrically to form continuous bands of elastic tissue to resist the wall tension from the arterial blood pressure. Because the tension in a pressurized cylinder increases in direct proportion to vessel diameter, it is necessary for animals to increase the thickness of the aorta as body size, and hence aortic diameter, increases. Wolinsky and Glagov (1967) showed that the thickness-to-diameter ratio of the aorta at mean arterial pressure remained constant at a value of 0.05 for a series of mammals of different sizes. The increase in thickness with size is achieved by the addition of apparently identical lamellar units, and this creates an aortic wall design in which the circumferential wall tension due to blood pressure is approximately 2 N per lamellar unit per metre of vessel length, regardless of animal size. One implication of this wall design is that the structure and properties of the mammalian lamellar unit appear to have been conserved through evolution in mammals, although there has never been a systematic investigation of this hypothesis. This leads us to the fundamental question addressed in this paper.

Although it is clear that the whale's aortic arch is much less stiff and much larger than its aorta, it is not clear whether the sizes of these vessels have been modified relative to those of normal mammals, or whether the structure and mechanical properties of their lamellar units have been modified. The analysis presented in this study will show that there have been significant changes in macroscopic dimensions through evolution, as well as changes in material properties due to major modifications in the architecture of the collagen fibre lattice.

Materials and methods

Arterial samples

Arteries were obtained during the summers of 1985 and 1986 at the whaling station at Hvalfjördur, Iceland. Fin whales (*Balaenoptera physalus* Lacépède) were delivered by catch boats to the whaling station within 24 h of death, and arterial samples were obtained during the 1–2 h flensing operation. Animals from which samples were obtained ranged in length from 17 to 20 m, and they were estimated to have body masses between 35 and 40 metric tons. Age determinations were not available. Following mechanical tests, arterial samples were preserved in 10 % formalin. Other samples were frozen for later analysis.

Collagen and elastin content

Elastin content was determined from the analysis of samples from two whales; one set of samples was collected in June 1985 and analyzed within 5 months, and the other was collected in June 1986 and analyzed within 9 months. Samples of arterial tissue were blotted and weighed to determine wet mass. They were then minced, freeze-dried and weighed to determine the dry mass and the total water content. Weighed portions of these dry samples were treated with 0.1 mol l^{-1} NaOH in a boiling water bath for 60 min to quantitatively isolate chemically pure elastin (Soskel *et al.* 1987). Purified elastin samples were then washed in distilled water, freeze-dried and weighed.

Collagen content was determined from amino acid analysis of samples of weighed, dry arterial wall from a single whale, collected in June 1986. Tissue was stored for 9 months prior to analysis. Samples of the arterial media were hydrolysed in 6 mol l^{-1} HCl at 105 °C, and amino acid analysis was carried out to determine the hydroxyproline content using a Beckman amino acid analyzer. Collagen content was calculated on the basis that hydroxyproline, at 109 residues per thousand, makes up 14 % of the mass of mammalian collagen (Miller, 1984). However, because elastin contains a small amount of hydroxyproline, it is necessary to correct for the hydroxyproline contribution from the elastin in each sample. Dolphin elastin contains 2.5 residues per 1000 hydroxyproline (Sage and Gray, 1979), making the elastin contribution quite small in the case of the thoracic and abdominal artery samples, but the very large elastin content of the aortic arch tissue made the corrections essential for reasonable determination of the collagen content.

Histology

Samples of arterial tissue were fixed in formalin at zero pressure, dehydrated in an alcohol series, embedded in wax, sectioned and stained with Verhoff's elastin stain and with picro-Ponceau (Humason, 1972). Other samples of formalin-fixed arterial media were washed in tap water, frozen and cryo-sectioned for inspection using a polarizing microscope, with or without a first-order red filter.

Tensile tests

Samples of whale aortic arch were dissected into rectangular strips, with the long axis oriented in the circumferential direction of the artery, for the preparation of samples that could be tested to reveal the circumferential stiffness of purified arterial elastin. The strips were autoclaved for 12 h (100 kPa, 120 °C) in order to produce a collagen-free and mechanically stable form of elastin (Partridge *et al.* 1955; Lillie *et al.* 1994). Tensile tests were conducted on an Instron 1122 tensometer, using pneumatic grips to hold the test strips, which were kept moist during the test period. The tissues were extended up to 75 % at a rate of $10\,\mathrm{mm\,min^{-1}}$ for several cycles of conditioning until repeatable responses were obtained. Force–extension data were used to calculate engineering stress σ_{eng}:

$$\sigma_{eng} = F/A_o\,, \tag{1}$$

where F is force (in N) and A_o is initial cross-sectional area (in m^2), and engineering strain ε_{eng} is given by:

$$\varepsilon_{eng} = \Delta L/L_0\,, \tag{2}$$

where ΔL is the change in sample length and L_0 is the initial length. Young's modulus (E), defined as:

$$E = \Delta\sigma_{eng}/\Delta\varepsilon_{eng}\,, \tag{3}$$

was calculated for the region of linear behaviour that occurred at strains above 0.3.

Purified elastin samples contain a mesh of elastin fibres and lamellae that are separated by water-filled spaces, which contained collagen and cells in the intact tissue. In order to obtain a cross-sectional area that does not include these spaces, we calculated true elastin cross-sectional area from measurements of elastin dry mass. That is, after testing, the sample was dried at 105 °C and weighed, and the hydrated mass was calculated by assuming that the elastin fibres contain 0.66 kg water per kilogram dry elastin (Lillie and Gosline, 1990). The hydrated volume was calculated, assuming a density of hydrated elastin of $1.18\times10^3\,\mathrm{kg\,m^{-3}}$, and the elastin cross-sectional area was determined by dividing the volume by the unstretched length of the hydrated test sample. This is the same procedure used to calculate the cross-sectional area of elastin in whole arteries from composition data (see hydrated volume estimates in Table 2); so even if the water content and density values are not precise, the predicted modulus based on this procedure will produce comparable results. Similar experiments were conducted on elastin rings isolated from pig thoracic aortas.

Results and discussion

Arterial dimensions and mechanical properties

In order to determine whether the aortic arch in the whale has been enlarged or whether the thoracic and abdominal aortas have been reduced, it is necessary to determine what vessel dimensions are appropriate for a mammal weighing 35–40 metric tons. Wolinsky and Glagov (1967) surveyed the diameters of thoracic aortas at mean arterial pressure for a series of terrestrial mammalian species ranging in size from a mouse (0.028 kg) to a pig (approximately 200 kg). In Fig. 1, the data from this study are shown on a log–log plot, and linear regression analysis indicates a highly significant power function relationship which can be expressed as:

$$d_a = 3.65M_b^{0.358}\ (r^2=0.95,\ P<0.001)\,, \tag{4}$$

where d_a is aortic diameter (in mm) and M_b is body mass (in kg). Fig. 1 shows this regression line, and extrapolation of this line to the body mass of a typical, 37.5 metric ton fin whale gives a predicted external diameter of the thoracic aorta of 158 mm. Inflation experiments described previously (Shadwick and Gosline, 1994) indicate that, at mean arterial pressure (estimated as 13 kPa), the external diameter of the thoracic aorta from an 18 m long male fin whale is approximately 130 mm. The measured value (square symbol in Fig. 1) falls well within the 95 % confidence interval of the regression line (dashed lines), and it appears that the external diameter of the thoracic aorta is in accordance with the dimensions seen in other mammals. This implies, therefore, that the aortic arch has been dramatically enlarged relative to the remainder of the arterial tree.

This conclusion, that the aortic arch is dramatically enlarged in the whale, is shown clearly in Fig. 2A. This figure gives the external arterial diameter along the length of the arterial tree to reveal the nature of the geometric taper in the major arteries

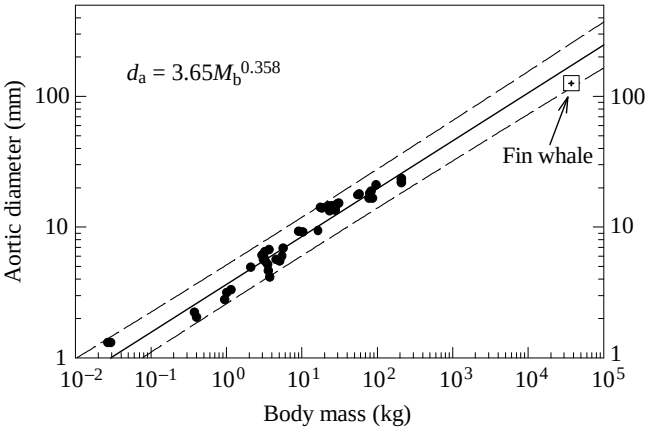

Fig. 1. Relationship between external aortic diameter (d_a) at mean arterial pressure and body mass (M_b). The data were digitized from a linear graph in Wolinsky and Glagov (1967) and log-transformed to establish the scaling relationship. The broken lines show the 95 % confidence limits of the prediction from this scaling relationship, and the single square symbol at a body mass of 37.5 metric tons gives the measured external diameter for a fin whale.

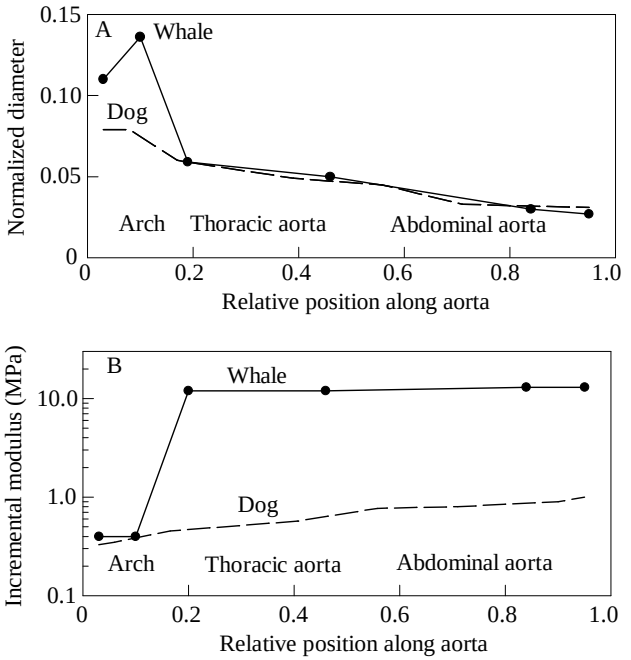

Fig. 2. Comparison of geometric taper (A) and elastic taper (B) for the fin whale (solid line and filled circles) and the dog (dashed line). In A, the external arterial diameter is normalized to the length of the thoracic aorta. In B, the incremental modulus values are from inflation tests at mean arterial pressure. The whale data are taken from Shadwick and Gosline (1994) and the dog data are from McDonald (1974) and Campbell *et al.* (1981).

of a fin whale and of a dog. The whale dimensions are based on measurements taken from a single, 17.7 m long female, and the dog dimensions were taken from two 20 kg dogs (McDonald, 1974; Campbell *et al.* 1981). For this comparison, the arterial diameter has been normalized by the length of the thoracic aorta (i.e. from the root of the arch to the diaphragm). The normalized diameters of the thoracic and abdominal aortas of the whale and the dog are remarkably similar along their entire length, and this confirms the conclusion above that the dimensions of the thoracic aorta seem appropriate for an animal of its size. The normalized diameter of the whale's aortic arch, however, is clearly different from that of the dog. The whale arch has nearly twice the normalized external diameter of the dog arch and, at the midpoint of the whale arch, the volume per unit length, based on internal dimensions, is about seven times that of the whale thoracic aorta. Indeed, this huge volume expansion in the whale arch is one of the key factors that allows the majority of the arterial compliance in the whale's central circulation to be located in the aortic arch. The other feature is the dramatic difference in the mechanical properties of the walls of the arch and the aorta.

Fig. 2B shows a comparison of the elastic taper of the arterial tree of a fin whale and of a dog. The modulus values are for the biaxial, circumferential, incremental modulus obtained from inflation tests at mean arterial pressure. In the arch region, the modulus of the whale elastic tissue is essentially identical to that of the dog, but in the thoracic and abdominal aortas there is an abrupt increase in the modulus of the whale tissue which makes this material about 30 times stiffer than that of the dog. The rise in modulus at this transition is probably even more abrupt than that indicated in Fig. 2B, as it appears to occur over a distance of about 10 cm, or less than 5 % of the total length of the thoracic aorta. In the thoracic and abdominal regions, the stiffness of the whale elastic tissue remains unchanged, but there is a gradual three- to fourfold increase in the modulus of the dog tissue, so that at the distal end of the arterial tree the whale:dog modulus ratio has fallen to about 10.

Taken together, the data in Fig. 2 suggest that the structural and developmental changes that have moulded the whale arterial tree have caused a dramatic enlargement of the arch region, but the similarity in mechanical behaviour suggests little change in the composition and structure of the lamellar units of which it is composed. In contrast, thoracic and abdominal aortas in the whale appear to have dimensions appropriate for the animal's size, but the very high stiffness of these vessels suggests a dramatic change in their composition and structure. Detailed analyses of vessel wall composition, mechanical properties and structure indicate that these preliminary conclusions do not tell the full story.

Connective tissue composition

Water content was determined for multiple samples from two whales, and constituted about 75 % of these tissues, as is typical of other mammalian arteries (McDonald, 1974). Specifically, the mean water content of the aortic arch (75±1.5 %, mean ± S.D., N=5) was not significantly different from that of the thoracic and abdominal aortas (73±3.3 %, N=13). Table 1 and Fig. 3 show the results of the connective tissue analysis of the aortic arch, and thoracic and abdominal portions of the descending aorta. The fibrous proteins elastin and collagen together account for 58–67 % of the tissue dry mass, and the major compositional difference between the three tissues is that the elastin:collagen ratio is much higher in the arch (approximately 2:1) than in the thoracic and abdominal aortas (approximately 1:2 and 1:3, respectively). This abrupt, fourfold change from elastin-dominated to collagen-dominated composition that occurs at the junction of the arch and the thoracic aorta parallels the form of the elastic

Table 1. *The elastin and collagen contents of whale arterial tissues*

	Arch (% dry mass)	Thoracic aorta (% dry mass)	Abdominal aorta (% dry mass)
Elastin	40±1.4 (N=4)	21±5.6 (N=2)	15±3.3 (N=5)
Collagen	21±12.7 (N=2)	46 (N=1)	43±6.2 (N=5)
Elastin + collagen	61	67	58
Elastin/collagen	1.9	0.46	0.35

Values indicate the mean value for the percentage of dry mass ± S.D. (N).

Data for elastin content are from two whales; data for collagen are from a single whale.

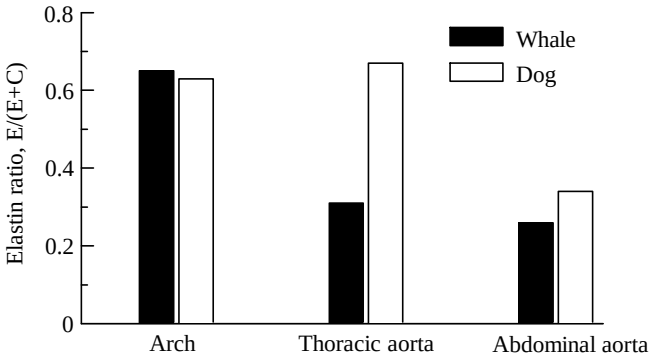

Fig. 3. Comparison of the elastin and collagen content in the major arteries of the fin whale (filled bars) and the dog (open bars). Composition is determined from dry mass content and expressed as the ratio of elastin (E) content to the sum of elastin plus collagen (C) contents. Data for the composition of dog arteries are from Milnor (1982).

taper illustrated in Fig. 2B, but these quantitative differences are not large enough to account for the 30-fold difference in incremental modulus (Fig. 2B) at this junction. This suggests that changes in wall structure as well as in wall composition are needed to explain the properties of these connective tissues. In contrast, the aorta of a dog shows a more gradual decrease in elastin content and increase in collagen content along the length of the descending thoracic and abdominal aortas (Fig. 3), such that compositional changes alone are sufficient to explain the observed threefold increase in incremental modulus (Fig. 2B).

Volume fractions of collagen and elastin

In order to assess the potential contributions of elastin and collagen to the tensile mechanical properties of the arterial tissues, the effective load-bearing cross-sectional area of each material must be known. This is not simply equivalent to their mass fractions because the hydration levels, and therefore density and volume, of collagen, elastin and cells differ. Using the dry mass fractions of collagen and elastin, we calculated the hydrated mass and volume occupied by each component (Table 2). These values are based on hydration factors (i.e. the ratio of hydrated to dry masses) of 1.66 for elastin and 2.5 for collagen (Shadwick, 1990) and on the density of dry protein being 1.33–1.4 g ml^{-1} (Lees, 1986). As an example of this procedure, consider that a 100 g sample of intact, hydrated aortic arch tissue, having a density of 1.07 g ml^{-1}, would occupy 93 ml. Since elastin makes up 40 % of the dry mass and the water content is 75 % by mass, this hydrated sample contains 10 g of dry elastin. Then, 10 g (of dry elastin) × 1.66 (hydration factor) equals 16.6 g of hydrated elastin, which should have a density of 1.18 g ml^{-1} and occupy a volume of 14.1 ml. This yields an elastin volume fraction, V_E, of 14.1/93=0.15. Collagen volume fractions, V_C, were calculated in the same manner, and the results for aortic arch and thoracic and abdominal aortas are given in Table 2. Note that the relationship between volume fraction and dry mass for elastin is different from that for collagen because of their different hydration factors (Tables 1, 2).

Table 2. *Volume fractions of hydrated elastin and hydrated collagen in the whale aorta and their potential effect on tensile circumferential stiffness of the vessel wall*

	Arch	Thoracic aorta	Abdominal aorta
Elastin volume fraction, V_E	0.15	0.08	0.06
Collagen volume fraction, V_C	0.12	0.28	0.27
Maximum Young's modulus due to elastin (kPa)	142	77	58
Maximum Young's modulus due to collagen (MPa)	160	380	370

Elastin and collagen contribution to arterial elasticity

Our tensile tests on elastin isolated from whale and pig aortas yielded similar results. In both cases, autoclave-purified elastin, when fully hydrated, was about 53 % by mass interfibrillar water and 47 % hydrated protein. The Young's modulus of elastin, E_E, calculated from tensile stresses based on the effective elastin cross section, was 950 kPa for whale elastin and 920 kPa for pig elastin. It should be noted that the estimate for the whale is based on the assumption that the protein hydration of whale elastin is identical to that of pig elastin, and therefore the near equivalence of these results should be viewed with some caution. However, there is no reason to expect that the hydration level of whale elastin differs significantly from that of pig elastin. These modulus values for pig and whale aortic elastin are slightly lower than the tensile stiffness of purified, single elastin fibres from bovine ligament (1.2 MPa; Aaron and Gosline, 1981) because in the mesh-like structure of the artery wall the elastin fibres are not oriented entirely in the circumferential direction. The method used in the current study compensates for the mesh structure and allows us to compute an effective, circumferential cross-sectional area. For the Young's modulus of collagen fibres, E_C, we used a value of 1.7 GPa, based on studies of mammalian tendon (Shadwick, 1990).

Next, we calculated the maximum artery wall stiffness that could be achieved for each vessel if the elastin fraction alone were responsible for resisting circumferential expansion under pressure. The effective, circumferential cross-sectional area of elastin was determined as above for the tensile test samples, from V_E, and the predicted stiffness was calculated as $E_E \times V_E$. This is 142 kPa for the aortic arch, and only 77 and 58 kPa for the thoracic and abdominal aortas, respectively (Table 2). To estimate the possible mechanical effect of full loading of the fibrous collagen component, we assumed that at maximal expansion the collagen fibres will be preferentially oriented to resist the circumferential wall tension. As a rough estimate, we

assume that the circumferential stiffness should be of the order of 80 % of the stiffness of parallel collagen fibres. Thus, the resulting maximum wall stiffness would equal $E_C \times V_C/1.25$. This is 160 MPa for the aortic arch but nearly 2.5 times greater in the thoracic and abdominal aortas (Table 2).

Stress–strain behaviour

The data in Fig. 2B provide only a very limited basis for comparing the elastic properties of arteries in the fin whale with those in other mammals. One extremely important property of arterial elastic tissues is that their stiffness (i.e. elastic modulus) must increase rapidly as an artery expands, and this implies a steeply rising, or J-shaped, stress–strain curve. The main role of rising stiffness is to prevent the formation of aneurysms (Burton, 1954; Roach and Burton, 1957; Gosline, 1980), which will occur for all cylindrical, elastic pressure vessels if the circumferential elastic modulus of the wall material remains constant. Typically, a mammalian aorta functions under physiological conditions at circumferential strains of around 0.5 (i.e. 50 % expansion), and the strain increases by 0.05–0.1 (5–10 %) with each heartbeat (Milnor, 1982; Armentano *et al.* 1991). Over this strain increment, the stiffness of the artery wall material rises about threefold, from about 200 kPa to about 600 kPa (Bergel, 1961).

Conventional dogma holds that the rubber-like protein elastin provides low-stiffness, long-range extensibility to the artery wall at low pressures and that as pressure increases in the physiological range the modulus rises because wall stress is gradually transferred to stiffer and stronger collagen fibres. There has, however, never been a complete assessment of artery wall properties in terms of collagen and elastin content and fibre architecture because the complexity of the fibre architecture makes an exact analysis extremely difficult. It appears that the wall stiffness at diastolic pressure is due to the elastin alone (Armentano *et al.* 1991), but this has not been verified quantitatively. The extreme difference between the tissues of the whale arch and aorta makes it possible for us to attempt a quantitative analysis, and this may provide insights into the design of the connective tissue fibre-lattices that control the subtle characteristics of shape in the stress–strain curves of arterial elastic tissues.

Fig. 4A shows stress–strain curves for the whale aortic arch, derived from results presented in Shadwick and Gosline (1994), but the data have been converted into engineering stress and engineering strain so that it is possible to calculate uniaxial Young's modulus values that can be compared with data from mechanical tests on isolated collagen and elastin samples. The open circles show circumferential stress–strain data from an untethered inflation experiment (i.e. biaxial test) that have been converted into uniaxial values by the methods of Dobrin and Doyle (1970) as described in Shadwick and Gosline (1994). The filled circles show data from a uniaxial, circumferential tensile test. It is clear that the stress–strain properties derived in these two different tests are very similar.

Fig. 4B shows Young's modulus values, obtained from the stress–strain data by taking the derivative of the regression equations described above. These modulus traces are plotted as the solid (uniaxial test) and broken (inflation test) lines. The vertical arrow indicates the circumferential strain produced by mean arterial pressure (i.e. 13 kPa) in the whale, and the physiological range of strains at pressures between 10 and 15 kPa is from 0.36 to 0.62. Over this strain increment of 0.26, the Young's modulus of the aortic arch material rises by about 50 %. This is quite unusual, as aortas typically show about a threefold increase in their circumferential, incremental modulus over a physiological extension of 10 % or less. Does this mean that the aortic arch will form aneurysms? Tests on the intact arch (Shadwick and Gosline, 1994) clearly show that it inflates uniformly along its length without forming aneurysms because the circumferential, incremental modulus of the wall material, which differs from the Young's modulus in that it takes into account the decline in wall thickness with expansion, rises at a rate that is sufficient to prevent the formation of aneurysms.

More interestingly, the modulus over the physiological range is extremely close to that predicted in Table 2 from the

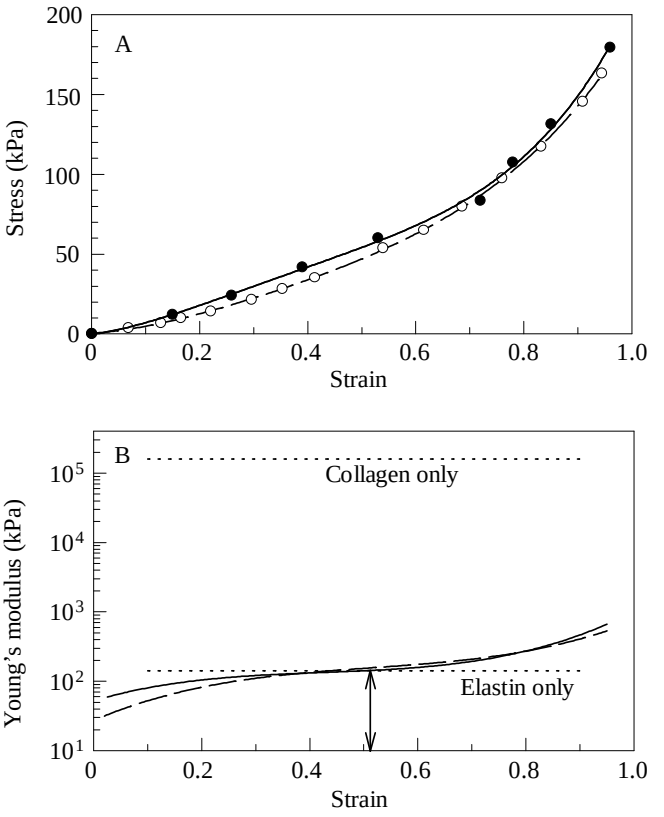

Fig. 4. Circumferential material properties of the fin whale aortic arch. (A) Engineering stress–strain data derived from inflation tests (open circles) and tensile tests (filled circles). The lines are fourth-order polynomial regressions. (B) The Young's modulus obtained by calculating the derivative of the regressions for the inflation test (broken line) and tensile test (solid line). The vertical arrow indicates the strain at mean arterial pressure (13 kPa) in inflation tests. Test data are from Shadwick and Gosline (1994). The dotted lines labelled collagen and elastin only are the moduli calculated for the collagen and elastin contents of the aortic arch (Table 2).

elastin content of the aortic arch (Fig. 4 dotted line, elastin only). Note that the predicted modulus coincides with the measured modulus at a strain that occurs between diastolic and mean arterial blood pressure. This means that at physiological pressures the wall tension in the aortic arch is supported almost entirely by elastin, and this is consistent with the observation that the elastin lamellae in an artery become straight at diastolic pressure (Wolinsky and Glagov, 1964). This is the first time that arterial properties have been predicted quantitatively from elastin content and properties, rather than from the assumption that the linear portion of the stress–strain curve at diastolic pressure arises entirely from straightened elastin lamellae (Armentano *et al.* 1991).

The Young's modulus falls at strains below the physiological range, presumably because the elastin lamellae are not straight, and thus the wall stress is not distributed evenly between all elements of the elastin mesh. At strains above the physiological range, the modulus of the material increases above that of elastin alone, and this is consistent with wall stress being transferred to collagen fibres. However, it is clear that this transfer is far from complete, even at strains well above the physiological range. The upper, horizontal, dotted line labelled 'collagen only' indicates the modulus expected from the collagen content of the aortic arch (Table 2). This prediction is based on the assumption that all collagen fibres are fully extended and thus carry load like the collagen fibres in a stretched tendon. Even at strains approaching 1.0 (i.e. 100 % extension), the modulus of the arch material is more than 100-fold lower than the prediction. Thus, the collagen fibres comprising 12 % of the wall volume (Table 2) are far from being fully extended. Without additional morphological information, it is not possible to reach definite conclusions about the architecture of the collagen fibre lattice, but it is very likely that this architecture is quite unusual because it allows such large-scale expansion with little stretching of the collagen fibres.

Fig. 5 shows a similar analysis for the thoracic aorta. The stress–strain data in Fig. 5A are derived from a tethered, circumferential inflation test (open triangles) and a uniaxial, circumferential tensile test (filled triangles) from Shadwick and Gosline (1994). Again, the data are converted to engineering stress and strain to facilitate comparison with data for elastin and collagen, and again the stress–strain curves from these two tests are very similar. Young's modulus values have been determined by finite difference over each interval of strain and are plotted in Fig. 5B using the same symbols. The strain at mean arterial pressure for the thoracic aorta is indicated by the vertical arrow, and the full physiological range of strain is between 0.425 and 0.441. That is, the physiological expansion of this artery is less than 2 %, and over this range the Young's modulus increases by about twofold. Again, we see unusual elastic properties over the physiological range, but in this case the high stiffness and corresponding lack of extension, as well as the small change in stiffness, suggest a material that is dominated by collagen.

The dotted lines in Fig. 5B show the mechanical behaviours

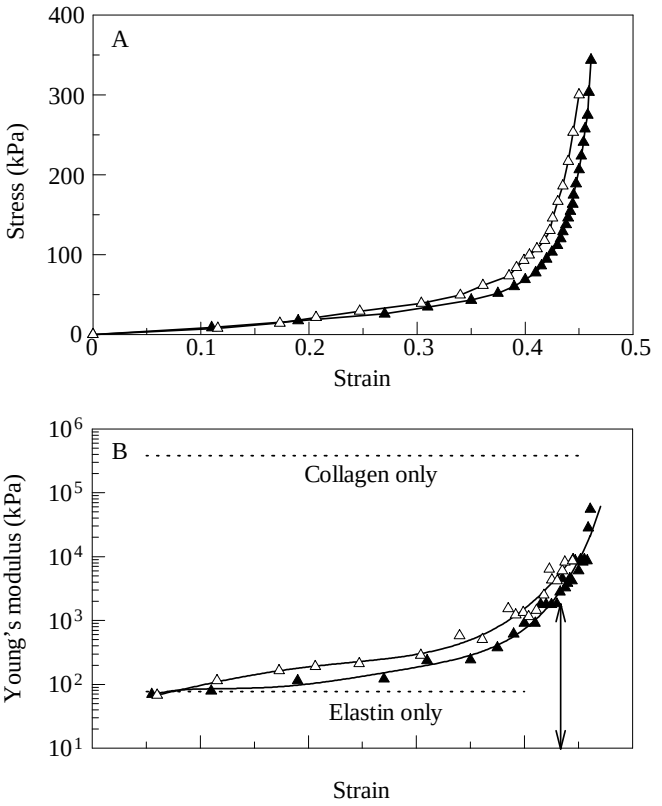

Fig. 5. Circumferential material properties of the fin whale thoracic aorta. (A) Engineering stress–strain data derived from inflation tests (open triangles) and tensile tests (filled triangles). (B) Young's modulus values calculated at each increment of strain. The lines are polynomial regressions fitted to the modulus data. The vertical arrow indicates the strain at mean arterial pressure (13 kPa) in inflation tests. Test data are from Shadwick and Gosline (1994). The dotted lines labelled collagen and elastin only are the moduli calculated for the collagen and elastin contents of the thoracic aorta (Table 2).

predicted from the elastin and collagen contents of the thoracic aorta (Table 2). The 'elastin only' line falls well below the modulus lines over almost all of the strain range, and it is lower by a factor of about 100 for the physiological range of strains. Thus, elastin has essentially no role in the physiological function of this artery, in spite of the fact that elastin occupies 8 % of the hydrated volume of the vessel wall. Surprisingly, even at very low strains, well below the physiological level, the thoracic aorta material has a Young's modulus that is two- to 30-fold higher than that predicted from its elastin content. Thus, in this unusual vessel, collagen carries the majority of the wall stress at strains that in 'normal' arteries are carried entirely by elastin.

The 'collagen only' line is well above the Young's modulus at mean arterial pressure, and this indicates that the vessel wall properties that determine its physiological function are not created by collagen fibres that are fully straightened and uniformly carrying wall stress in the physiological range. The rapid transition from low stiffness to high stiffness, which starts at a strain of about 0.40 (Fig. 5B), makes the stress–strain curve for the thoracic aorta look remarkably like that for a

tendon. Tendons are tensile, rope-like structures constructed from bundles of parallel collagen fibres, but the fibres are crimped rather than perfectly straight. As a consequence, tendons show a J-shaped stress–strain curve in which modulus rises in a toe region that extends to strains of 0.03–0.1 (3–10 % extension) before the collagen fibres are extended and the tendon enters the linear region of high-stiffness behaviour (Diamant *et al.* 1972; Fung, 1993). Interestingly, at the highest strains achieved in the inflation and tensile tests, the thoracic aorta material reached Young's modulus values that were about one-quarter that expected for fully extended, tendon collagen fibres. The test results presented in Fig. 5 were limited by the size and strength of the apparatus and transducers used in these tests. If the tests could have been continued to failure, it is likely that higher modulus values would have been observed. Considering the similarity between the properties of the thoracic aorta and tendons, it is probable that the thoracic aorta contains tendon-like, crimped fibres, and polarized light microscopy will confirm this.

Structure of the lamellar units in artery wall elastic tissues

Figs 6 and 7 show the morphology of elastic tissues from the thoracic aorta and the aortic arch at the light microscope level. Figs 6A and 7A show bright-field images of cross sections stained to reveal the elastin lamellae, which appear as dark, horizontal lines. All mammalian arteries contain elastin lamellae (stained black in these sections), which are separated by layers of collagen fibres (stained light red) and by smooth

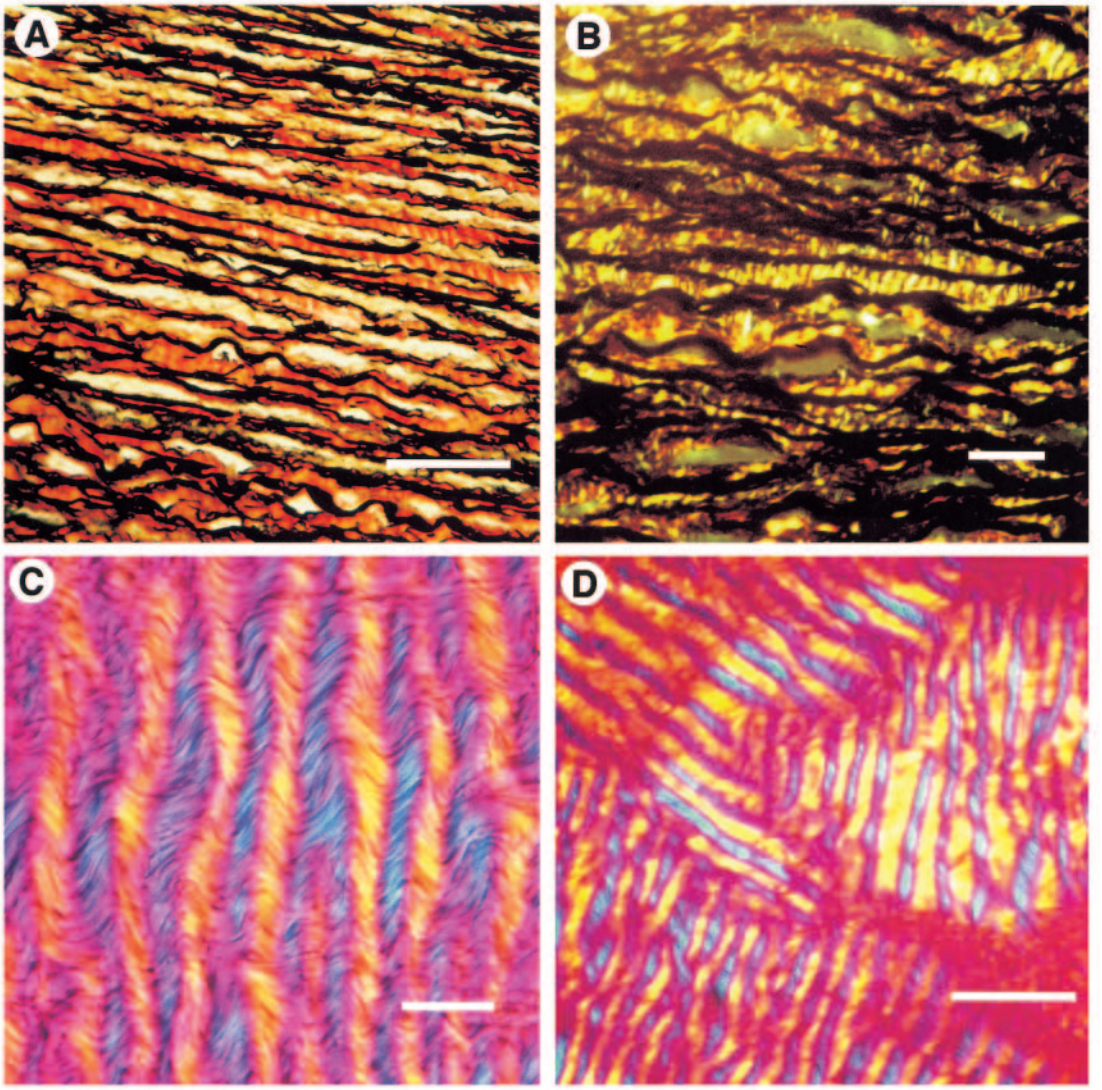

Fig. 6. The structure of the lamellar units in the fin whale thoracic aorta. (A) Bright-field view of a cross section stained to reveal the elastin lamellae, which appear as dark, horizontal bands. Scale bar, 100 μm. (B) Polarized light view of a stained cross section at higher magnification to demonstrate the organization of the lamellar unit, with collagen fibre bundles (yellow), elastin lamellae (black) and muscle cells (light brown). Scale bar, 25 μm. (C) Polarized light view of a tangential section taken with a first-order red filter, revealing bands of collagen fibres that run in the plane of the section. The pattern of wavy collagen fibres within the collagen bundle is clearly visible. Scale bar, 20 μm. (D) Polarized light view of a tangential section with a first-order red filter showing three wide bundles of collagen fibres running in different directions in the plane of the section. The horizontal fibre bundle in this figure runs in the circumferential direction in the aorta. Scale bar, 100 μm.

muscle cells (stained light brown) to form lamellar units. The current model for the lamellar unit (Clark and Glagov, 1985) contains four layers (muscle cell – elastin – collagen – elastin), rather than just muscle–collagen layers alternating with elastin lamellae, as was originally thought (Wolinsky and Glagov, 1964).

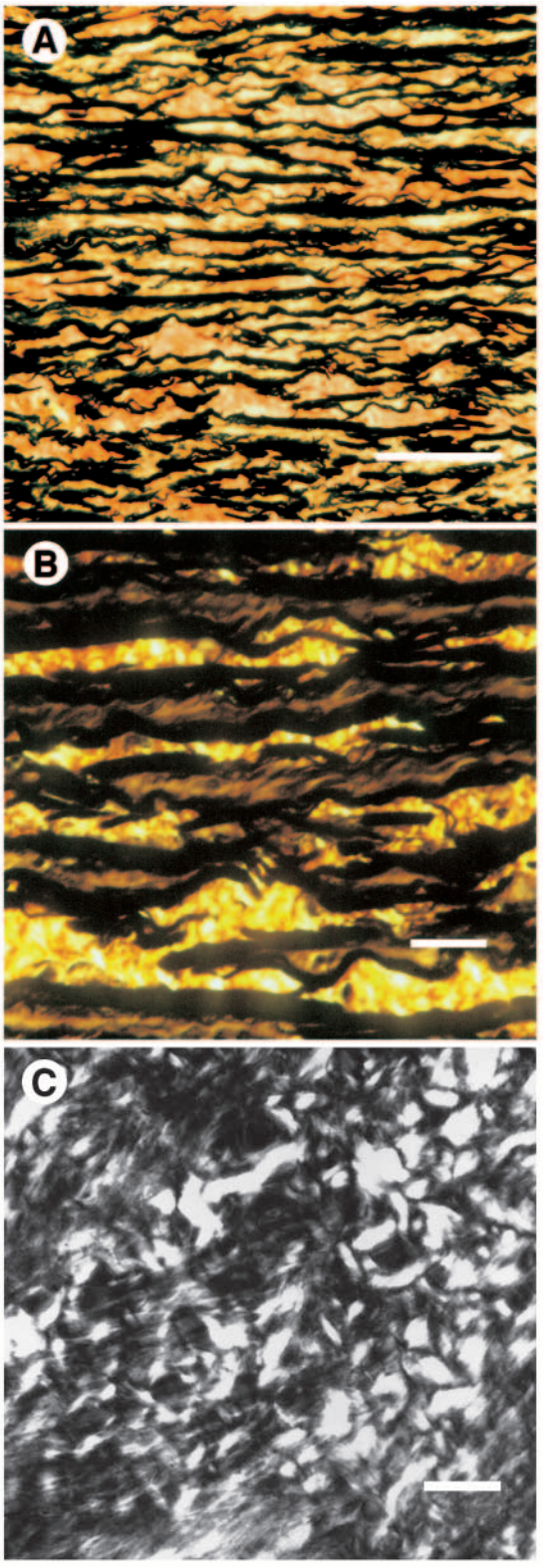

The relationships derived by Wolinsky and Glagov (1967) for the diameter, thickness and number of lamellar units of the thoracic aorta as a function of body size allow us to predict the wall thickness and lamellar number for the whale thoracic aorta and possibly also for the whale aortic arch. The wall thickness:diameter ratio should be 0.05, and lamellar units should be 15 μm thick, giving approximately 65 lamellae per millimetre of wall thickness at mean arterial pressure. The thoracic aorta of the whale has a predicted external diameter of 15.8 cm at mean arterial pressure and, thus, the predicted thickness of 0.79 cm should contain 510 lamellar units. If the arch fits the pattern established for aortas of other animals, then the whale aortic arch, with a measured external diameter at mean arterial pressure of about 37 cm, should be 1.85 cm thick and should contain about 1200 lamellar units.

Measurements of these parameters are listed in Table 3. Wall thickness and external diameter values were obtained from the results of inflation experiments described in Shadwick and Gosline (1994). The thoracic aorta has a thickness:diameter ratio of 0.015, which is less than one-third of the expected value. The lamellar number for the thoracic aorta (170±11, N=10), obtained by counting the number of dark elastin bands across the full thickness of the vessel wall at several locations, is much less than expected for a vessel with an external diameter of 13 cm, and the consequence of the low lamellar number is that the tension per lamellar unit (4.8 N m^{-1}) is 2.5 times greater than expected. The lamellar units, however, are of normal thickness. For a thoracic aortic wall thickness at mean arterial pressure (13 kPa) of 0.21 cm and total lamellar number of 170, lamellar thickness is between 12 and 13 μm.

The aortic arch has a thickness:diameter ratio of 0.055, which is similar to the expected value. The total lamellar number for the aortic arch was obtained by dividing the arch wall thickness by the mean thickness of lamellar units. Mean lamellar thickness (55±5 μm, N=6) was obtained from measurements of 10–20 lamellar units at several locations through the thickness of the arch wall in frozen sections that spanned the full wall thickness. For a wall thickness of 4.5 cm and a mean lamellar thickness of 55 μm, the total lamellar number is about 820. When the arch is strained to its *in vivo* state, wall thickness becomes 1.95 cm, and therefore lamellar thickness at mean arterial pressure is about 24 μm, a value that is considerably larger than predicted. The tension per lamellar

Fig. 7. The structure of the lamellar units in the fin whale aortic arch. (A) Bright-field view of a cross section stained to reveal the elastin lamellae, which appear as dark, horizontal lines. Scale bar, 100 μm. (B) Polarized light view of a cross section at higher magnification to demonstrate the organization of the lamellar unit, with collagen fibre bundles (yellow), elastin lamellae (black) and muscle cells (light brown). Scale bar, 25 μm. (C) Polarized light view of a tangential section showing short segments of collagen fibre bundles that emerge from the plane of the section at steep angles. This indicates their radial orientation in the wall of the arch. The section is about 12 μm thick. Scale bar, 25 μm.

Table 3. *Structural scaling in the aorta of an 18 m long fin whale*

	Aortic arch		Thoracic aorta	
	Predicted	Measured	Predicted	Measured
Diameter (cm)		37	15.8	13
Thickness (cm)	1.85	1.95	0.79	0.21
Thickness:diameter	0.05	0.055	0.05	0.015
Lamellar thickness (μm)	15	24	15	13
Total lamellar number	1200	820	510	170
Total wall tension (N m^{-1})	2400	2150	1020	820
Tension per lamella (N m^{-1})	2	2.6	2	4.8

All dimensions are referenced to an inflation pressure of 13 kPa.

Predicted values are derived from allometric data taken from Wolinsky and Glagov (1967). Measured values for external diameter, wall thickness and thickness:diameter ratio come from inflation tests (Shadwick and Gosline, 1994). See text for further details of the measurements for lamellar thickness and total lamellar number.

Circumferential wall tension per unit vessel length is defined as pressure × internal radius.

unit in the arch (2.6 N m^{-1}), although slightly above the average expected value, is well within the range observed by Wolinsky and Glagov (1967).

These comparisons of expected and measured lamellar properties reveal two important features. The lamellar units in the thoracic aorta carry higher tension than expected, and the lamellar units in the arch are thicker than expected. The micrographs in Figs 6A,B and 7A,B give a hint of the changes that have occurred in the lamellar structure of whale arteries. The thoracic aorta (Fig. 6A,B) has normal-looking lamellar units near the inner surface, in which all four layers of muscle, elastin and collagen are arranged as suggested by the model of Clark and Glagov (1985), However, very little muscle tissue is visible over the majority of the thickness of the aorta, and it appears that muscle spaces are largely filled by thick layers of collagen. The lamellar units in the aortic arch (Fig. 7A,B) have the normal complement of four layers throughout the thickness of the wall, but the lamellar unit is thickened by elastin lamellae that are very thick (approximately 5–7 μm in Fig. 7B, which would make them approximately 4 μm at mean arterial pressure) and by an unusually thick collagen layer.

The distribution of the collagen layers is shown clearly in the high-magnification, polarized light micrographs in Figs 6B and 7B. These sections have been stained for elastin, collagen and muscle, as above, but the ordered molecular structure of collagen makes collagen fibres highly birefringent in polarized light and thus easy to identify. In the thoracic aorta (Fig. 6B), the yellow collagen bands are separated by very dark elastin lamellae. In the aortic arch section (Fig. 7B), the collagen fibres appear as yellow areas between the very dark, horizontal elastin lamellae and somewhat lighter smooth muscle cells. The elastic tissues from both the thoracic aorta and the arch contain large amounts of collagen, but this conclusion is at odds with the results of the stress–strain analysis, which suggested that the thoracic aorta is very strongly dominated by collagen but that the arch material is much less collagen-dominated than normal arteries. The only way that this apparent contradiction can be explained is if the structure of the collagen fibre-lattices in the aorta and the arch are very different.

Architecture of the collagen fibre lattice

In the thoracic aorta, the bands of collagen have an appearance that is nearly identical to that of the crimped collagen fibres that exist in tendons. The long yellow stripe at the centre of Fig. 6B is a large bundle of collagen fibres whose orientation is nearly parallel to the plane of this section and thus is maximally birefringent. Since this is a cross section, this collagen bundle runs in a circumferential direction within the artery wall. Collagen bundles at different locations in this cross section appear less birefringent and extend for shorter distances in the section because their orientation is different. Longitudinal fibre bundles would not be visible in this section because collagen fibres are not birefringent when observed end-on, and bundles oriented at some intermediate angle, winding helically around the axis of the aorta, would appear as short, birefringent segments.

Returning to the circumferential fibre bundle at the centre of Fig. 6B, note the pattern of bright and dark bands. This banding pattern arises from the wavy path that individual collagen fibres follow within the fibre bundle. This wavy structure is revealed more clearly in Fig. 6C, which shows a tangential section of a single bundle of collagen fibres at high magnification. The colour in this figure arises from the use of a first-order red filter that makes it much easier to distinguish the direction of molecular orientation in a complex birefringent object. Areas of the field that are pink have little or no birefringence, and in this case pink coloration indicates areas occupied by elastin or regions of collagen fibres that run parallel to the polarizer or analyzer (i.e. vertical or horizontal in this figure). Birefringent areas are coloured either yellow or blue, depending on the local orientation of the collagen fibres relative to the polarizer–analyzer axis. The collagen fibres have an overall orientation that runs horizontally in this figure, but where the fibres run downwards to the left they appear blue, and where they run upwards to the left they appear yellow. This

picture clearly establishes that the overall direction of collagen fibres in these wavy bundles runs at right angles to the blue and yellow stripes. Fig. 6C also allows us to visualize the wavelength and wave amplitude of the waves present in the fibre bundles. The fibres appear to have a diameter of about 1–2 μm, and the wavelength is about 15–20 μm in this bundle. The large amplitude of the wave indicates that these collagen fibre bundles must be stretched to large extensions before the fibres are straightened and the bundle approaches maximal stiffness. Indeed, inflation tests (Shadwick and Gosline, 1994) indicate that *in vivo* the thoracic aorta is stretched longitudinally by 22 % through its tethering to the skeleton and is expanded circumferentially by at least 40 %. Thus, the waviness apparent in this figure will be substantially reduced *in vivo*.

Fig. 6D shows, at lower magnification, a nearly tangential section that passes through three lamellar units and reveals collagen bundles that run in three different directions. This section was cut in approximately the outer 10 % of the medial layer, where the density of collagen fibres is somewhat higher than in the central layers, and it was selected to show the different orientations that can occur in the vessel wall. Sections taken towards the centre of the artery wall would be similar, but the range of fibre orientation within any single section would not be as wide as that in Fig. 6D. However, the relative densities of collagen and elastin are similar, and the full range of fibre orientations that occur in the mid-wall of the artery is greater than that shown in Fig. 6D.

Taken together, these micrographs indicate a collagen fibre architecture in the whale thoracic aorta that is different from that observed in other mammals. Wavy collagen fibre arrays exist in other arteries (Ling and Chow, 1977; Clark and Glagov, 1985; Canham *et al.* 1991), but elastin-rich thoracic aortas do not normally contain such wide expanses of wavy collagen fibres that are locked in such close register. It seems likely, therefore, that one important feature of the design of this vessel is that all the collagen fibres have a similar wave pattern, so that the modulus can rise quickly over a very narrow range of strain (see Fig. 5). In this sense, the aorta is very tendon-like in its construction. If individual fibre bundles had very different wave patterns, then some would become taut at low strains while others would become taut only at large strains, and this would spread the rise in stiffness over a broad range of strain. However, the aorta is loaded biaxially, whereas a tendon is loaded in uniaxial tension. Thus, a tendon has all its crimped fibre bundles running parallel to each other, while the fibre bundles in the aorta run in many directions to resist both longitudinal and circumferential wall stresses. It is likely, therefore, that the precise orientation of the collagen fibre bundles is also of considerable importance. If all, or at least most, fibre bundles are to carry the wall stress equally and allow the wall stiffness to rise rapidly, then there should be a close matching of the fibre waviness and the bundle orientation to achieve the tendon-like material properties.

The situation in the aortic arch seems to fall at the other extreme. Stress–strain properties indicate a material whose stiffness rises very slowly with increasing strain, and thus precisely ordered bands of uniformly wavy collagen bundles are very unlikely. The polarized light micrographs in Fig. 7B,C show that this is indeed the case. The yellow, birefringent areas in the arch cross section (Fig. 7B) may seem to have a similar appearance to that of the thoracic aorta, but this is definitely not the case. At several locations it is possible to observe bright bands that appear to run at large angles relative to the orientation of the elastin lamellae. This shows that some collagen bundles run in a direction that has a radial component of orientation within the arch wall. These collagen bundles are not the same as the tendon-like bands seen in the aorta, which arise from crimped or wavy collagen fibres in tight arrays. The collagen fibre bundles in the arch actually have a component of radial orientation, and this can be demonstrated by careful observation under the polarizing microscope. If the cross section is rotated, these fibre bundles go dark when they are aligned with the polarizer or analyzer axis, and this process clearly reveals that the majority of collagen fibres in the aortic arch have a significant radial component of orientation.

The radial orientation of the collagen is seen more clearly in tangential sections. Fig. 7C shows a tangential section in normal polarized light, without the first-order red filter, because the arch material is dominated by non-birefringent elastin and muscle, and it would appear almost entirely pink with the filter. The bright collagen fibre bundles stand out clearly from the dark elastin and muscle-rich areas. The most important feature of this micrograph is that all the bright areas (collagen fibre bundles) are very short, indicating that the collagen bundles pass through the plane of this section at fairly steep angles. It is clear that the collagen bundles all have a significant radial component to their orientation, and therefore many, or perhaps most, of the collagen fibres run in directions which would allow them to attach one elastin lamella to another in the radial direction. This section, however, comes from a sample that was fixed without pre-stretch to the *in vivo* state. At mean arterial pressure, the arch will be expanded by about 50 % in both the circumferential and longitudinal direction, and thus, the collagen fibre bundles will be oriented much closer to the tangential plane *in vivo*. It remains likely, however, that the collagen and elastin units in the arch material are arranged in series, rather than running parallel to one another, as is apparently the case for the whale thoracic aorta and for lamellar units in other aortas. The series models proposed by Brown *et al.* (1994) for the organization of elastin and collagen in the highly extensible wing ligaments of birds may provide insights into the organization of the whale aortic arch, but these wing ligaments all show a rapid rise in stiffness that is associated with the transfer of wall stress to a collagen fibre lattice that ultimately runs in parallel with the elastin fibres. The failure of the whale aortic arch material to show a sharp rise in stiffness, even at very high biaxial strains, suggests a unique organization that remains to be explained in detail.

Significance of the results

This study provides clear documentation of dramatic modifications that have occurred in the evolution of the fin whale central arterial tree. These modifications include changes to vessel dimensions and dramatic changes in the structural organization of the lamellar unit of the vessel wall. The aortic arch is larger than expected for an animal of its size, but the ratio of wall thickness to vessel diameter appears normal. However, at the microscopic level, the lamellar units show a marked change in both the thickness of elastin lamellae and in the organization of the collagen fibre-lattice. The possibility that collagen and elastin may be arranged in series would explain the unusually large expansion of the arch and the small rise in the elastic modulus over the physiological range of pressure, properties that allow this vessel to form the major compliance structure in the whale's circulatory system. However, the details of the organization of the lamellar unit remain to be determined. The thoracic aorta appears to have an appropriate external diameter, but the wall thickness and lamellar number are much smaller than expected. As a consequence, the tension per lamellar unit is higher than the norm for mammals. The mechanical behaviour indicates a tendon-like material that is dominated by collagen, behaviour that is appropriate for a non-compliant vessel. The microscopic structure reveals collagen fibre bundles that are very tendon-like in their organization. Again, the details of collagen fibre waviness and orientation remain to be determined.

It is important to note that the microscopic data presented in this paper were obtained from material that was fixed without a trans-luminal pressure to hold the connective tissue elements in the orientation that occurs at normal physiological pressures. Since both the arch and the aorta undergo considerable circumferential and longitudinal strain to reach their *in vivo* dimensions, the collagen fibre orientations that determine the physiological properties will be quite different from those shown in our micrographs. Before we can fully understand the structural basis for the mechanical properties of these arterial tissues, it will be necessary to establish the structure in a series of vessels that have been perfusion-fixed at a range of pressures that span the physiological range. However, it may be particularly difficult to obtain this information for whale arteries. The whale's aortic arch has a volume of about 60 l and a wall thickness of nearly 2 cm at mean arterial pressure; perfusion fixation could be a major challenge!

To date, no one has been able to explain the mechanical properties of any elastic artery in terms of the three-dimensional organization of its collagen fibre-lattice. Attempts using X-ray diffraction to determine the distribution of collagen fibre orientation in pig thoracic aorta (Roveri *et al.* 1980) failed because X-ray diffraction cannot distinguish the long-range orientation of a collagen fibre from the local orientation associated with fibre waviness. This approach was successful in predicting the properties of dried arteries (Bigi *et al.* 1981), but in dried arteries the non-collagen matrices stiffen to form a rigid fibre-reinforced composite in which there is no possibility of wavy collagen fibres straightening with applied load. Thus, differences between fibre orientation and fibre waviness are immaterial in dried arterial tissue. However, in hydrated tissue, the difference between fibre orientation and waviness is important, and it must be quantified before mechanical properties can be predicted. Canham *et al.* (1991) showed that it is possible to use quantitative polarized light microscopy with a three-dimensional stage to document the orientation and waviness of collagen fibres in cerebral and coronary arteries fixed at physiological pressures. When this type of information becomes available for whale arteries or for other elastic arteries, mathematical models that relate mechanical properties to elastin fibre and collagen fibre distribution functions, such as the one produced by Lanir (1979) for skin, will allow us to address some of the structural issues raised in this study and may provide a full, quantitative explanation for the mechanical behaviour of these unique blood vessels.

The authors acknowledge the generous assistance provided by Kristian Loftsson of Hvalur and by the many workers at their whaling station in Hvalfjördur, Iceland. We also thank Steve Wainwright, Paul Brodie, Lisa Orton, Ann Pabst and John Long for assistance during the field work. This study was supported by research grants from the Natural Sciences and Engineering Research Council of Canada to J.M.G. and from the University of California Faculty Exchange Program.

References

AARON, B. B. AND GOSLINE, J. M. (1981). Elastin as a random-network elastomer: a mechanical and optical analysis of single elastin fibers. *Biopolymers* **20**, 1247–1260.

ARMENTANO, R. L., LEVENSON, J., BARRA, J. G., FISCHER, E. I. C., BREITBART, G. J., PICHEL, R. H. AND SIMON, A. (1991). Assessment of elastin and collagen contribution to aortic elasticity in conscious dogs. *Am. J. Physiol.* **260**, H1870–H1877.

BERGEL, D. H. (1961). The static elastic properties of the arterial wall. *J. Physiol., Lond.* **156**, 445–457.

BIGI, A., RIPAMONTI, A., ROVERI, N., JERONIMIDIS, G. AND PURSLOW, P. P. (1981). Collagen orientation by X-ray pole figures and mechanical properties of media carotid wall. *J. Materials Sci.* **16**, 2557–2562.

BROWN, R. E., BUTLER, J. P., ROGERS, R. A. AND LEITH, D. E. (1994). Mechanical connections between elastin and collagen. *Connective Tissue Res.* **30**, 295–308.

BURTON, A. C. (1954). Relation of structure to function in the tissues of the walls of blood vessels. *Physiol. Rev.* **34**, 619–642.

CAMPBELL, K. B., RHODE, E. A., COX, R. H., HUNTER, W. C. AND NOORDERGRAAF, A. (1981). Functional consequences of expanded aortic bulb: a model study. *Am. J. Physiol.* **240**, R200–R210.

CANHAM, P. B., TALMAN, E. A., FINLAY, H. M. AND DIXON, J. G. (1991). Medial collagen organization of human arteries of the heart and brain by polarized light microscopy. *Connective Tissue Res.* **26**, 121–134.

CLARK, J. M. AND GLAGOV, S. (1985). The transmural organization of the arterial media; the lamellar unit revisited. *Arteriosclerosis* **5**, 19–34.

DIAMANT, J., KELLER, A., BAER, E., LITT, M. AND ARRIDGE, R. G. C. (1972). Collagen: ultrastructure and its relation to mechanical properties as a function of ageing. *Proc. R. Soc. B* **180**, 293–315.

DOBRIN, P. B. AND DOYLE, J. M. (1970). Vascular smooth muscle and the anisotropy of dog carotic artery. *Circulation Res.* **27**, 105–119.

DRABEK, C. M. (1975). Some anatomical aspects of the cardiovascular system of some antarctic seals and their possible functional significance in diving. *J. Morph.* **145**, 85–106.

FUNG, Y. C. (1993). *Biomechanics: Mechanical Properties of Living Tissues*. New York: Springer Verlag. 568pp.

GOSLINE, J. M. (1980). The elastic properties of rubber-like proteins and highly extensible tissues. In *The Mechanical Properties of Biological Materials* (ed. J. F. V. Vincent and J. D. Currey). *Symp. Soc. exp. Biol.* **34**, 331–357. Cambridge: Cambridge University Press.

HUMASON, G. L. (1972). *Animal Tissue Techniques*. 3rd edn. San Francisco: W. H. Freeman and Co.

LANIR, Y. (1979). Rheological behaviour of the skin: Experimental results and a structural model. *Biorheology* **16**, 191–202.

LEES, S. (1986). Water content in type I collagen tissues calculated from the generalized packing model. *Int. J. biol. Macromol.* **8**, 66–72.

LILLIE, M. A., CHALMERS, G. AND GOSLINE, J. M. (1994). The effects of heating on the mechanical properties of elastin. *Connective Tissue Res.* **31**, 23–35.

LILLIE, M. A. AND GOSLINE, J. M. (1990). The effects of hydration on the dynamic mechanical properties of elastin. *Biopolymers* **29**, 1147–1160.

LING, S. C. AND CHOW, C. H. (1977). The mechanics of corrugated collagen fibrils in arteries. *J. Biomech.* **10**, 71–77.

MCDONALD, D. A. (1974). *Blood Flow in Arteries*. London: Edward Arnold. 496pp.

MILLER, E. J. (1984). Chemistry of the collagens and their distribution. In *Extracellular Matrix Biochemistry* (ed. K. A. Piez and A. H. Reddi), pp. 41–81. New York: Elsevier.

MILNOR, W. R. (1982). *Hemodynamics*. Baltimore: Williams and Wilkins. 390pp.

PARTRIDGE, S. M., DAVIS, H. F. AND ADAIR, G. S. (1955). The chemistry of connective tissues. II. Soluble proteins derived from partial hydrolysis of elastin. *Biochem. J.* **61**, 11–21.

ROACH, M. R. AND BURTON, A. C. (1957). The reason for the shape of the distensibility curves of arteries. *Can. J. Biochem. Physiol.* **35**, 681–690.

RODIN, J. A. G. (1980). The architecture of the vessel wall. In *Handbook of Physiology*, section 2, no. 2, *The Cardiovascular System*, vol. II, *Vascular Smooth Muscle*. Bethesda, MD: American Physiological Society, pp. 1–31.

ROVERI, N., RIPAMONTI, A. AND PULGA, C. (1980). Mechanical behaviour of aortic tissue as a function of collagen orientation. *Makromol. Chem.* **181**, 1999–2007.

SAGE, H. AND GRAY, W. R. (1979). Studies on the evolution of elastin. I. Phylogenetic distribution. *Comp. Biochem. Physiol.* **64**B, 313–327.

SHADWICK, R. E. (1990). Elastic energy storage in tendons: mechanical differences related to function and age. *J. appl. Physiol.* **68**, 1033–1040.

SHADWICK, R. E. AND GOSLINE, J. M. (1994). Arterial mechanics of the fin whale suggest a unique hemodynamic design. *Am. J. Physiol.* **267**, R805–R818.

SHADWICK, R. E. AND GOSLINE, J. M. (1995). Arterial windkessels in marine mammals. In *Biological Fluid Dynamics* (ed. C. P. Ellington and T. J. Pedley). *Symp. Soc. exp. Biol.* **49**, 243–252. Cambridge: Company of Biologists Ltd.

SOSKEL, N. T., WOLT, T. B. AND SANDBERG, L. B. (1987). Isolation and characterization of insoluble and soluble elastins. In *Methods in Enzymology*, vol. 144, *Structural and Contractile Proteins*, part D, *Extracellular Matrix* (ed. L. W. Cunningham), pp. 196–214. Orlando: Academic Press, Inc.

WOLINSKY, H. AND GLAGOV, S. (1964). Structural basis for the static mechanical properties of the aortic media. *Circulation Res.* **14**, 400–413.

WOLINSKY, H. AND GLAGOV, S. (1967). The lamellar unit of aortic medial structure and function in mammals. *Circulation Res.* **20**, 99–111.